

# Optimization Techniques for Fault Identification in Rotor Dynamics

**Ricardo Corrêa Simões**

Federal University of Uberlândia  
[rcsimoes@mecanica.ufu.br](mailto:rcsimoes@mecanica.ufu.br)

**Valder Steffen Júnior**

Federal University of Uberlândia  
[vsteffen@mecanica.ufu.br](mailto:vsteffen@mecanica.ufu.br)

*Abstract. This paper presents a methodology to detect and locate faults in rotor shafts. The damage presence diminishes the stiffness of the rotor then the vibrational behaviour is altered. The fault identification is dealt as an engineering inverse problem and the fault parameters (position, severity, length) are the system inputs to be found. A functional formed by the difference between the dynamic characteristics of the system and the model is minimized for identification purposes. Genetic algorithms were chosen to perform the optimisation task. Results of computational simulation show a good correlation between simulated fault parameters and identified ones.*

*Keywords: Flexible rotors, cracked shaft, fault detection, inverse problem, genetic algorithms*

## 1. Introduction

Nowadays The modern design of rotating machinery increases the use of composite materials and new alloys in various machine components. These materials permit rotating machinery to attain high operation speeds. However, such materials are susceptible to the appearance of fault. These faults lead to a loss of mechanical properties of the materials reducing fatigue life, which can cause the machine to fail or to the malfunction of its components.

A sudden failure in rotating machinery can cause great economic loss, inconvenience to users and even loss of human lives. To avoid such problems it is necessary to develop a methodology to detect the faults at their early stages. The trend of increasing the use of thermal plants for energy generation in Brazil is a factor that reinforces the necessity of the national industry to develop fault detection techniques.

In the mid-seventies a great number of publications about rotors containing faults (most transverse cracks) have been published. According to Muszynka (1982), at least 28 rotor failure faults that can be attributed to shaft crack, occurred during the period 1972 to 1982 in the North-American utility industry. Several researchers propose mathematical models to represent rotors with cracks: Gasch (1976), Henry and Okae-Avae (1976) and Mayes and Davies (1976). Nelson and Nataraj (1986) use the F.E.M. ( Finite Element Method) to represent more realistic complex industrial rotors. Cheng and Ku (1991) simulate the dynamic behaviour of a damaged rotor, regarding the fault as a source of energy reduction. This reduction entails modification in the element stiffness matrix.

The opening and closing crack mechanism due to the shaft rotation is known as “breathing”. The breathing phenomenon introduces non-linearities in the rotor properties and alters the shaft stiffness periodically with its rotation. Nelson and Nataraj (1986) use truncate Fourier series to represent mathematically the crack open/close mechanism. Bachschmid and Tanzi (2001) propose that the breathing mechanism and the vibratory motion of the cracked rotor are influenced by thermal stress, that can appear during thermal transients when machine operation conditions change. The breathing phenomena will not be discussed in the present work.

The purpose of this work is to evaluate the changes in the dynamic properties of flexible rotors (natural frequencies, eigen-modes, critical speeds and unbalance response) due to the presence of faults in the shaft. The fault is characterized by three parameters: severity (related with fault depth), position along the shaft, and length.

The identification of the fault parameters is based on Genetic Algorithm techniques. The functional to be minimized is composed by the difference between the dynamic characteristics of the system and those from a F.E.M. model. The fault parameters are the design variables to be obtained through the optimization program. Genetic Algorithms were used in the present work due their robustness in solving inverse-problems in engineering.

## 2. Theoretical Background

### 2.1. Equations of Motions

Flexible rotors are dynamical systems whose models are composed typically by elements such as flexible shafts, rigid discs and bearings. The equation that describes the motion of the rotor can be obtained by applying Lagrange’s equation, Eq.(1), to energy expressions calculated for the rotor elements. More detailed information about the rotor equations of motion can be found in Lalanne and Ferraris (1998).

$$\frac{d}{dt} \left( \frac{\partial T}{\partial \dot{q}_i} \right) - \frac{\partial T}{\partial q_i} + \frac{\partial U}{\partial q_i} = Fq_i \quad (1)$$

where  $q_i$  are generalized independent coordinates,  $Fq_i$  are generalized forces and  $T$  and  $U$  are the kinetic and strain energy components, respectively.

The disc elements are assumed as being rigid and have only kinetic energy. Shaft elements are elastic systems having both kinetic and strain energy. The shaft finite element is shown in Fig.(1): the element has 2 nodes, each node has 4 degrees of freedom namely, 2 translations ( $u, v$ ), and 2 rotations ( $\theta, \psi$ ).

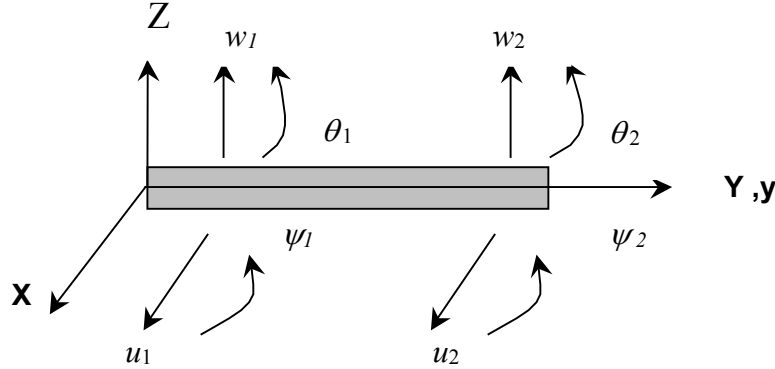


Figure 1. Degrees of freedom of shaft finite element.

The degrees of freedom of the shaft element can be arranged into two different vectors,  $\delta u$  (displacement along  $X$  direction) and  $\delta w$  (displacement along  $Z$  direction), Eq.(2) and Eq. (3), respectively.

$$\delta u = [u_1, \psi_1, u_2, \psi_2]^T \quad (2)$$

$$\delta w = [w_1, \theta_1, w_2, \theta_2]^T \quad (3)$$

The displacements  $u$  and  $w$  can be approximated by:

$$u = N_1(y) \delta u \quad (4)$$

$$w = N_2(y) \delta w \quad (5)$$

where  $N_1(y)$  and  $N_2(y)$  are cubic shape functions for a bending beam. The relations between displacements and slopes are:

$$\theta = \frac{\partial w}{\partial y} \quad (6)$$

$$\psi = -\frac{\partial u}{\partial y} \quad (7)$$

The kinetic ( $T_s$ ) and strain ( $U_s$ ) energies of a shaft element are given by the following expressions:

$$T_s = \frac{\rho I}{2} \int_0^L \{(\dot{\theta})^2 + (\dot{\psi})^2\} dy + \frac{\rho S}{2} \int_0^L \{(\dot{u})^2 + (\dot{w})^2\} dy - 2I\rho\Omega \int_0^L \psi \theta dy + \rho I L \Omega^2 \quad (8)$$

$$U_s = \frac{E \cdot I}{2} \int_0^L \left[ \left( \frac{\partial^2 u}{\partial y^2} \right)^2 + \left( \frac{\partial^2 w}{\partial y^2} \right)^2 \right] dy \quad (9)$$

where  $I$  is the area moment of inertia of the shaft cross section,  $S$  is the cross section area,  $\rho$  is the density and  $L$  is the element length. Substituting displacement equations and their derivatives into Eq.(8) and Eq.(9) and using the Lagrange's equations in the resulting equations, one obtains the classical mass ( $M$ ), the secondary mass ( $M_s$ ), the gyroscopic ( $C$ ) and the stiffness ( $K$ ) matrices of shaft elements (Lalanne and Ferraris (1998)) .

## 2.2. Fault model

The crack diminishes the area moment of inertia of the rotor cross section in which the fault is localized. Therefore, shaft stiffness decreases and the rotor vibratory pattern alters. The area moments of inertia about X axis ( $I_x$ ) and Z axis ( $I_z$ ) change from a maximum to minimum value during a rotation cycle, depending on the angular position of the fault. This behaviour introduces non-linearity in the cracked rotor.

A simplified fault model considers an average value of the area moment of inertia of the damaged cross section along a rotation cycle ( $I_d$ ).  $I_d$  is related to the no faulty area moment of inertia,  $I$ , by using a parameter  $\xi$ , Eq.(10), where  $\xi$  represents damage severity. Deeper cracks generate smaller values to  $\xi$ .

$$I_d = \xi I \tag{10}$$

This model considers that the shaft possesses a localized damaged region and, for that region, the deterioration is assumed to be uniform per unit length and distributed in such a way that no shift in the line of action of the resultant force occurs, Cheng and Ku (1991). Then, the corresponding damaged finite element has less capacity to store strain energy with respect to an undamaged element. The damaged element is considered to have a length  $L_d$ , which is supposed to be as small as possible in order to represent a realistic fault. As the fault is localized at an arbitrary location along the shaft, its location is associated with the position of the damaged element ( $p$ ) along the shaft. Thus, three parameters are used to characterize the fault. This way, a vector of design variables,  $V_p$ , can be formed for optimization purposes, as given by Eq.(11):

$$V_p = [\xi, p, L_d] \tag{11}$$

## 3. Fault identification using optimization methods

Usual methods to identify faults in structures, such as ultrasonic, infrared radiation, magnetic particles, are not effective in dealing with rotors due the existence of high noise levels found in industrial plants. Moreover, the necessity to stop the plant to conduct the tests is a time-consuming operation and causes economic losses. As vibration patterns reflect changes in mechanical properties of a structure, they can be used to identify and localize damage.

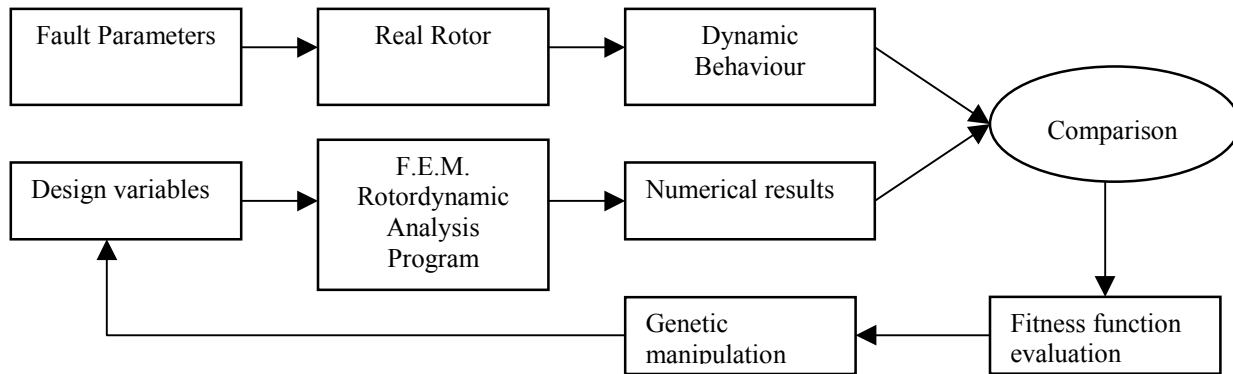


Figure 2. Scheme of inverse problem solution.

The determination of physical parameters of structures by using system output signals (vibration signals in the present case) is treated in engineering as an inverse problem, He et al (2001). The solution of the inverse problem demands two principal components: a simulation F.E.M. rotordynamic analysis program and a non-linear optimization code. Figure (2) illustrates the scheme of an inverse problem solution by using genetic algorithms in the optimizer.

The identification process is written as an optimization problem in which the minimization of a functional formed by the difference between the dynamic characteristics of the real system and the dynamic characteristics of the F.E.M. model. At the end of the process it is reasonable to expect that the functional will be minimized (global minimum) and the design variable values are such that they correspond to the fault parameters of the real mechanical system.

### 3.1. Genetic algorithms

Classical optimization techniques present good performance in dealing with well defined objective functions, in which the gradient is easily obtained all over the design variable domain. However, it is well known that classical methods fail in solving most inverse problems found in dynamics. Moreover, classical optimization techniques can not deal with local minima that also are prone to appear in such kind of task. Genetic Algorithm techniques have the advantage of not using gradient information and they are not influenced by local minima.

Genetic algorithms are probabilistic search algorithms that imitate natural selection processes and genetics. An initial population of individuals (solutions) is randomly created. Each individual in this initial population is evaluated and, according to its fitness, survives or is eliminated. The chosen ones are copied to perform genetic manipulations, according to crossover and mutation. Again, the “best” individuals are chosen and the process is repeated until a convergence criterion is achieved, Michalewicz (1994). The scheme of a simple genetic algorithm is shown in Fig.(3).

Two classes of Genetic Algorithms can be implemented. Both of them follow the same sequence of modeling genetic recombination and natural selection. The first represents parameters as an encoded binary string and the other works directly with continuous parameters (floating numbers), Haupt and Haupt (1998). Figure (4) shows a chromosome individual representation using binary encoding.

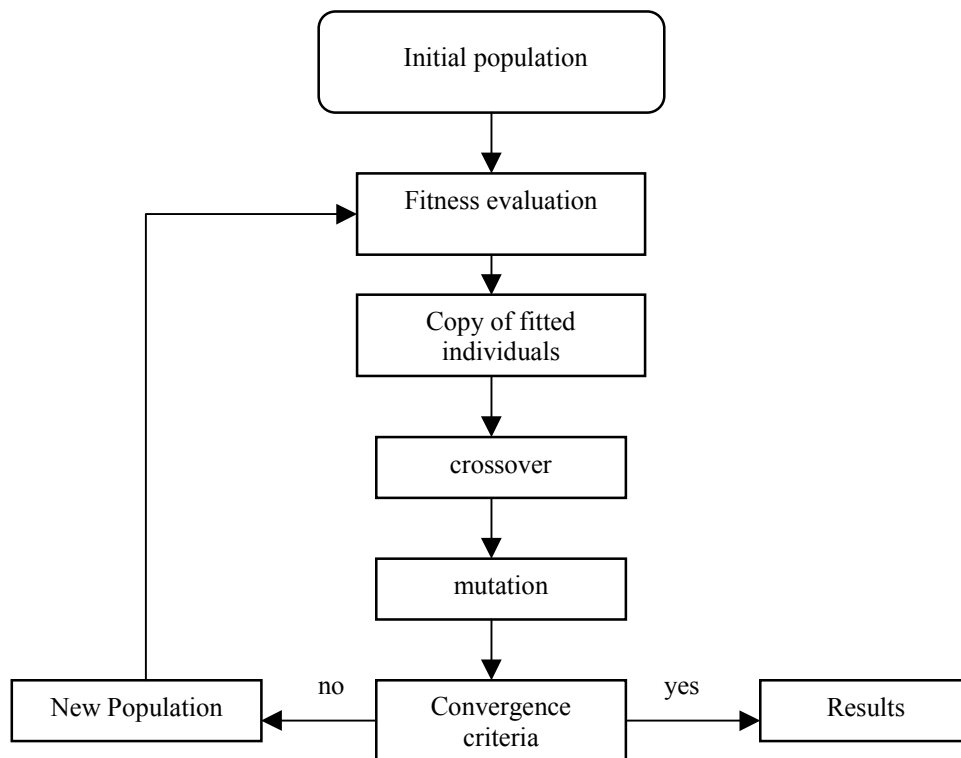


Figure 3. Simple genetic algorithm flowchart.

#### 3.1.1. Genetic operators

In the following, the most important genetic operators are briefly described.

**Selection:** The selection of individuals that will be copied into the next generation is done in the way that higher fitness individuals have their survival chances increased. There are several selection processes: roulette wheel and its extensions, scaling techniques, tournament, elitist models, and ranking methods, according to Goldberg (1989) and Michalewicz (1994).  
**Crossover:** During this operation two new individuals are generated by the changing of genetic material between two individuals that are randomly chosen, Fig.(5). Parents are eliminated from the population in such a way that the number of individuals remains constant.

**Mutation:** Mutation process alters a small allele quantity of the entire population. Mutation tries to hold genetic diversity among the individuals and avoids fast convergence.

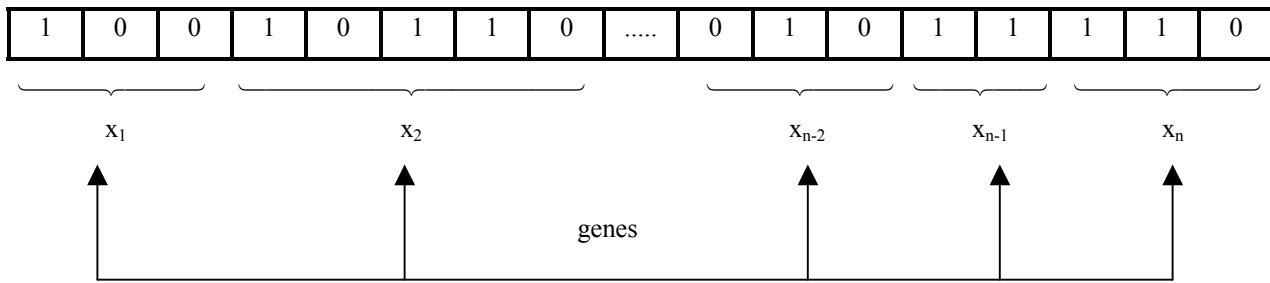


Figure 4. Representation of an individual in binary code.

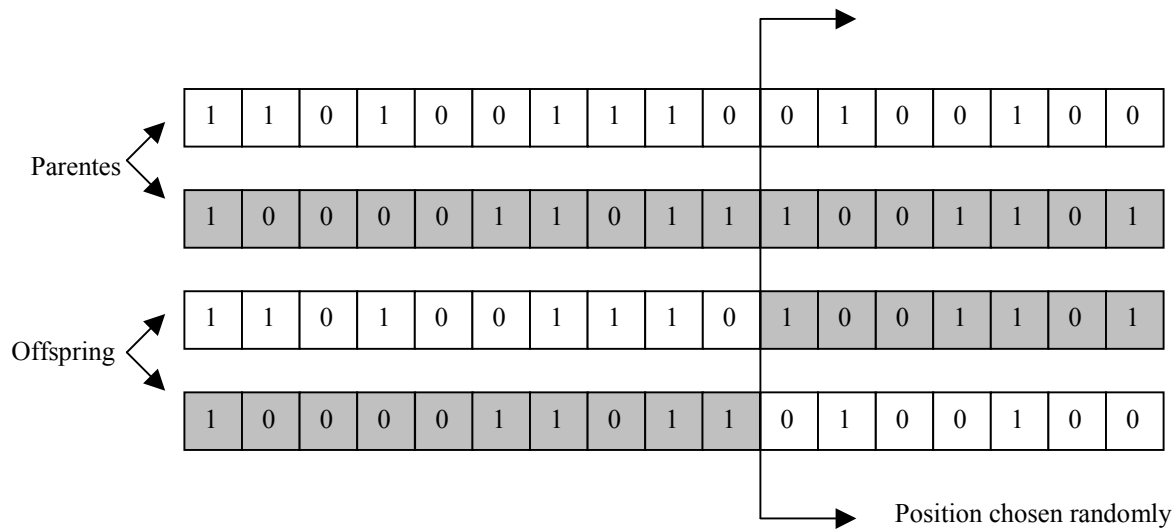


Figure 5. Binary crossover.

#### 4. Dynamic response of cracked rotors

The dynamic behaviour of cracked rotors was studied by analyzing the influence of the three fault parameters (severity, location, length) on the rotor response. Four dynamic features were analyzed, aiming at obtaining meaningful information about fault influence: whirl speed, vibration modes, unbalance response and critical speeds. The dynamic response of a vertical rotor model, composed by a 10 mm diameter shaft, three discs and two support bearings localized at the ends, as shown in Fig.(6). The physical properties of the discs are presented in Tab.(1) and the bearing properties are shown in Tab.(2). To simulate the dynamic behaviour of the rotor-bearing system, the program MONOROTOR was used (developed at INSA Lyon-France).

Table 1. Physical properties of discs.

Disc	Mass(Kg)	Moment of Inertia (Kg m <sup>2</sup> )	Polar Moment of Inertia (Kg m <sup>2</sup> )	External Diameter (m)	Thickness (m)
Inferior	0.963	0.0008	0.0017	0.12	0.011
Central	1.51	0.0021	0.0043	0.15	0.011
Superior	0.784	0.0004	0.0008	0.09	0.016

Table 2 . Physical properties of bearings.

Bearing	$K_{xx}$ (N/m)	$K_{zz}$ (N/m)
Lower	18,774	18,774
Upper	24,774	24,774

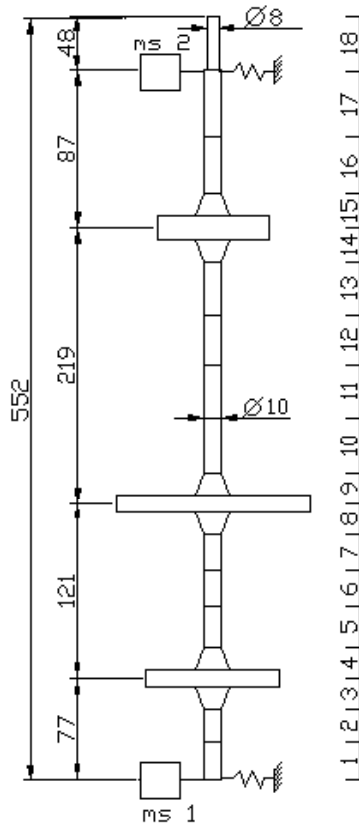


Figure 6. Vertical rotor F.E.M. model.

The influence of fault severity in whirl speeds is shown in Fig.(7). It is observed that more severe faults causes greater reductions in whirl speeds, as it was expected. Figure (8) shows the influence of damage location in whirl speeds. It can be observed that the fault localized at the 10th finite element (see Fig.(6)) leads to greater changes than faults localized in another position. It is worth to mention that this position corresponds to the maximum displacement point for the third mode. The fault does not affect significantly the rotor vibration modes, Fig.(9), however the modes determine which whirl speed will be the most affected by damage. Table (3) shows the results for the third critical speed of the rotor. The position  $p = 10$  is the one that most alters the critical speeds in the present example. More detailed analysis about the influence of fault parameters in the rotor dynamic behaviour can be found in Simões (2002).

Table 3. Third critical speed.

Damage severity ( $\xi$ )	Critical speed (Hz)		
	Damage location		
	$p = 5$	$p = 10$	$p = 12$
0.5	49.02	48.18	48.84
0.8	49.31	49.09	49.29
1	49.41		

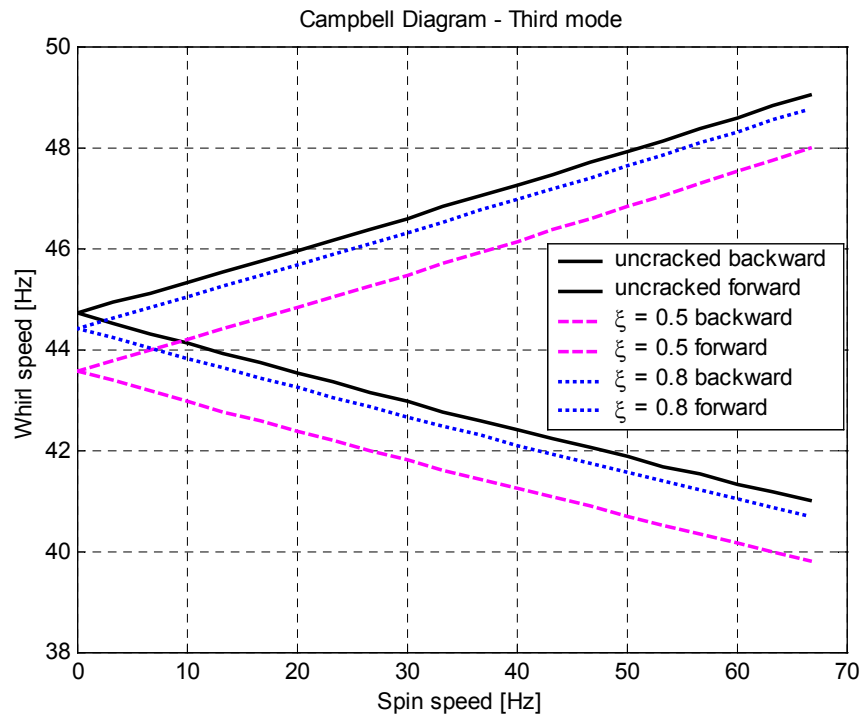


Figure 7. Whirl speeds of the cracked rotor,  $p = 10$ ;  $L_d = 0.01$  m.

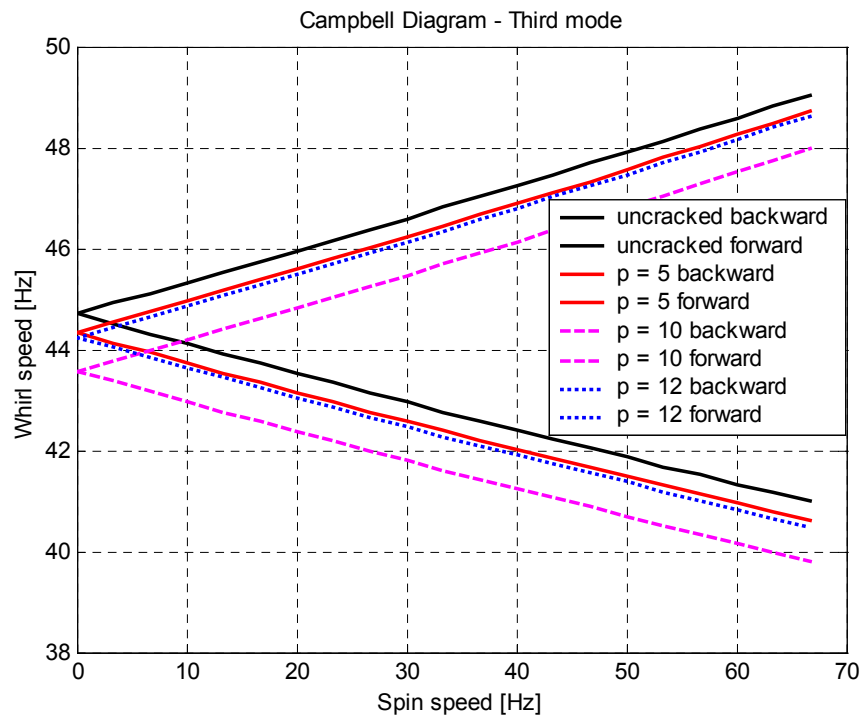


Figure 8. Whirl speeds of the cracked rotor,  $\xi = 0.5$ ;  $L_d = 0.01$  m.

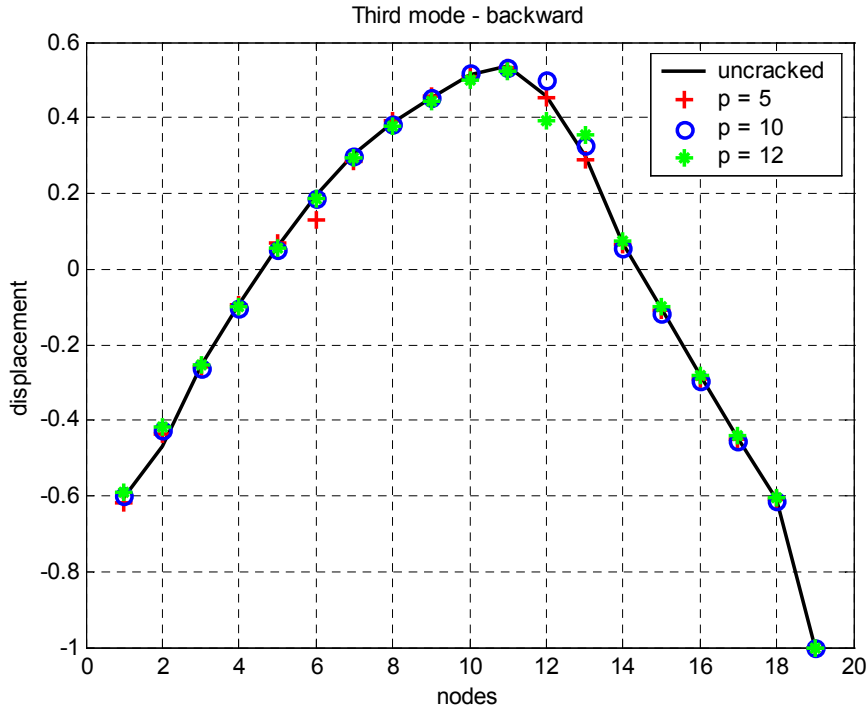


Figure 9. Third mode - backward,  $\xi = 0.5$ ;  $L_d = 0.01$  m.

## 5. Simulation results.

A set of files containing the dynamic characteristic of the rotor was obtained by using MONOROTOR program. The fault parameters were previously established in such a way that the corresponding results play the role of the real system. The code GAOT version 5 (The Genetic Algorithm Optimization Toolbox for Matlab 5) was used for optimization (this software was developed in the College of Engineering - North Carolina State University – USA).

The fault parameters (vector  $V_p$  - Eq.(11)) are optimized by coupling the program MONOROTOR with the code GAOT. For this purpose, it is necessary to define lower and upper bounds to the design variables, write the objective function to be minimized, define the initial population and its size, and fix the number of generations. As the optimization code was designed to maximize a fitness function, the negative of that function is set. The fitness function is given by Eq.(12):

$$F_{obj} = \sum_{j=1}^6 w_j^q \cdot \left( \sum_{i=1}^n (\omega_i^S - \omega_i^m)^2 \right)_j + \sum_{i=1}^3 w_j^r \left( (Vc^S - Vc^m)^2 \right)_j + \sum_{j=1}^6 w_j^S \cdot \left( \sum_{i=1}^1 (S_i^S - S_i^m)^2 \right)_j + w^t \cdot \sum_{i=1}^k (d^S - d^m)^2 \quad (12)$$

where  $\omega^S$  are vectors corresponding to the first six whirl speeds of the “real” system,  $S^S$  correspond to the first six modes,  $d^S$  is the vector that contains the unbalance response of the system and  $Vc^S$  are the first three critical speeds. The vectors  $\omega^m$ ,  $S^m$ ,  $d^m$  and the value  $Vc^m$  represent the same dynamic quantities as above, for the mathematical model.  $w_j^q$ ,  $w_j^r$ ,  $w_j^S$  e  $w^t$  are weight coefficients used in the multi-objective function. Finally, in Eq.(12)  $n$  corresponds to the discretization used in the determination of the whirl speeds,  $l$  is the number of nodes in the F.E.M. mesh and  $k$  is the number of unbalance responses calculated.

The simulation results obtained for the rotor presented in Fig.(6) are shown in Tab.(4). The size of the initial population was 1000 individuals and the number of generation was fixed to 15. The average calculation time was 3 hours, running in a PC-Athlon 1200 MHz computer. The situation in which two simultaneous faults are considered together along the rotor was also analyzed, as shown in Tab.(5). In that case, the size of the initial population remained the same as before.



Table 4. Simulation results (one fault along the rotor).

Simulation	"Real" parameter			Identified parameter			Objective function
	$\xi$	p	$L_d(m)$	$\xi$	p	$L_d(m)$	
1	0.5	6	0.02	0.45	6	0.017	0.0756
2	0.5	13	0.02	0.423	13	0.015	0.0918
3	0.5	17	0.02	0.542	17	0.024	0.0857
4	0.8	4	0.02	0.836	4	0.026	0.089
5	0.8	11	0.02	0.894	11	0.04	0.077
6	0.8	11	0.02	0.894	11	0.017	0.077
7	0.5	5	0.002	0.51	5	0.0021	$6.5 \cdot 10^{-5}$
8	0.5	10	0.002	0.55	10	0.0025	$1.1 \cdot 10^{-4}$

Table 5. Simulation results (two simultaneous faults along the rotor).

Simulation		Fault parameters						Objective function
		Fault 1			Fault 2			
		$\xi$	p	$L_d(m)$	$\xi$	p	$L_d(m)$	
1	Real parameters	0.5	6	0.003	0.8	12	0.003	$1.7 \cdot 10^{-4}$
	Identified parameters	0.53	6	0.0035	0.82	12	0.0034	
2	Real parameters	0.5	5	0.003	0.8	10	0.003	0.004
	Identified parameters	0.7	5	0.006	0.78	10	0.0035	
3	Real parameters	0.5	5	0.005	0.5	13	0.005	0.0058
	Identified parameters	0.64	5	0.0035	0.5	13	0.0044	

The fault location along the shaft was the parameter that was estimated with better accuracy, followed by the fault severity, and finally the fault length, as shown in the Tab.(4) and Tab.(5). This was expected because fault location is the parameter that most influences the dynamical behaviour of the system, as shown in the results of section 4. The identification of two simultaneous faults is a harder task, duplicating the number of parameters required by the optimization process.

## 6. Conclusions

The analysis of the dynamic behaviour of cracked rotors showed that fault location is the most sensitive parameter, followed by fault severity and fault length, Fig.(8). Only severe faults introduce considerable changes in the vibratory behaviour of the rotor, Tab.(3) and Fig.(7). This aspect justifies difficulties that appear in fault identification procedures. Whirl speeds are more sensitive to damage than mode shapes, Fig.(7), Fig.(8) and Fig.(9). Identified fault parameters presented good agreement, (mainly fault location, with respect to real parameters, as shown in Tab.(4) and Tab.(5). Future work shall include non-linear fault behaviour in the rotor model in order to represent more realistic situations.

## 7. References

- Bachschmid, N. and Tanzi, E., 2001, "Vibration Pattern Related to Transverse Cracks in Rotors", Proc. XVI Brazilian Congress of Mechanical Engineering, Vol 10, pp. 505-511.
- Cheng, L. M. and Ku, D. M., 1991, "Whirl Speeds and Unbalance Response of a Shaft-Disk System with Flaws", The International Journal of Analytical And Experimental Modal Analysis, Vol 6, No 4, pp. 279-289.
- Goldberg, D. E., 1989, "Genetic Algorithms in Search, Optimization, and Machine Learning", Addison-Wesley Publishing Company, Inc. USA.

- Gasch, R., 1976, "Dynamic Behaviour of a Simple Rotor with a Cross-Sectional Crack", Institution of Mechanical Engineers Conference Publication, Vibration in Rotating Machinery, Paper No. C178/76, pp. 123-128.
- Haupt, R.L. and Haupt, S.E., 1998, "Practical Genetic Algorithms", John Wiley and Sons, New York.
- He, Y., Guo. D. and Chu, F., 2001, "Using Genetic Algorithms To Detect and Configure Shaft Crack For Rotor-Bearing System", Computer Methods in Applied Mechanics And Engineering, 190, 5895-5906.
- Henry, T. A. and Okah-Avae, B. E., 1976, "Vibration in Cracked Shafts", Institution of Mechanical Engineers Conference Publication, Vibration in Rotating Machinery, Paper No. C178/76, pp. 15-19.
- Lalanne, M. and Ferraris, G., 1998, "Rotordynamics Prediction in Engineering", 2nd Edition, John Wiley and Sons, New York.
- Mayes, I. W. and Davies, W. G. R., 1976, "The Vibration Behaviour of a Rotating Shaft System Containing a Transverse Crack", Institution of Mechanical Engineers Conference Publication, Vibration in Rotating Machinery, Paper No. C178/76, pp. 53-64.
- Michalewicz, Z., 1994, "Genetic Algorithms + Data Structures = Evolution Programs", Third Edition, AI Series, Springer-Verlag, New York.
- Muszynka, A., 1982, "Shaft Crack Detection", Seventh Machinery Dynamics Seminar, Canada.
- Nelson, H. D. and Nataraj, C., 1986, "The Dynamics of a Rotor System with a Cracked Shaft", ASME Journal of Vibration, Acoustics, Stress, and Reliability in Design, Vol 108, pp. 189-196.
- Simões, R. C., 2002, "Fault Identification in Flexible Shaft of Rotors by Using Optimization Techniques" (in Portuguese), MSc Thesis, Federal University Of Uberlandia, Uberlandia ,MG, Brazil, October.